Recurrent Neural Network as Estimator for a Virtual sEMG Channel

Juliano C. Machado, Vinicius H. Cene and Alexandre Balbinot, *Member, IEEE.*

Abstract— **This study aims at estimating a virtual surface Electromyography (sEMG) channel through a Recurrent Neural Network (RNN) by using Long Short-Term Memory (LSTM) nodes. The virtual channel is used to classify hand postures from the publicly NinaPro database with a multi-class, one-against-all Support Vector Machine (SVM) using the Root Mean Square RMS of the sEMG signal as feature. The classification of the signals through the virtual channel was compared with uncontaminated data and data contaminated with noise saturation. The hit rate from the clean data has averaged 73.96% ± 3.02%. The classification from the contaminated data of one of the channels has improved from 9.29% ± 4.42% to 66.48% ± 6.11% with the virtual channel.**

I. Introduction

Many motor rehabilitation researches focus on the functional recovery of the amputated hand or arm. Superficial electromyography (sEMG) and pattern recognition (PR) algorithms for prosthesis control have been widely studied in the last decades in order to offer a practical way of controlling the different degrees of freedom in such prosthesis [1], [2], [3] but none of this techniques have so far shown commercial advantages. This kind of algorithm has a simple limitation: none of the proposed methods could include all the necessary criterion to be accept by the patients, such as natural and intuitive control, real-time system, adaptive parameters and configurations, little or none training stage, few electrodes, and other limitation factors [4]. Hence, many studies focusing on making sEMG-PR based prosthesis with intuitive and intelligent control, and not only on high PR accuracy, are being developed [5], [6], [7].

Recent advances in the sEMG signal processing and surgical methods, such as target muscular reinnervation (TMR) [8], provide some solutions for sEMG-PR based systems. In the signal processing area, some studies have shown a relationship in the arm kinetic and sEMG signal [9], [10] and many adaptive approaches [11], [12], [5].

The Recurrent Neural Network (RNN), defined by [13], is specialized in time series data, with supervised training [14] and, just as others neural networks, it fits nonlinear models. This kind of network uses iterative cyclic in the hidden layer to store information about the last states by using memory nodes [15]. One known issue of the RNN are the so called "long-term dependencies" caused by the fact that all layers share the same weights, making it difficult to learn how to store information in a very long sequence [16]. To solve this problem, a memory cell called Long Short-Term Memory (LSTM) has been proposed [17].

The LSTM is a memory node belonging to the RNN's hidden layer, as shown in Fig. 1. It should be noted that the LSTM has three additional inputs – or gates – in addition to the data from the input layer. They are called input gate, output gate and forget gate [18] and control the data flow. The input gate uses data from the input layer and from other cells outputs to scale the update contribution to the state cell from the input layer. The output gate uses the same kind of input data used by the input gate but to scale the output from the state cell. Scales are made by a sigmoid activation function that multiplies the data by a value between 0 and 1. The forget gate is used to make the cell maintain or forget the state and it was proposed by [18] considering that the state could enter in saturation during long series, making it difficult to predict long time series.

Figure 1: Example of an RNN-LSTM with two LSTM in the hidden layer. Adapted from [15].

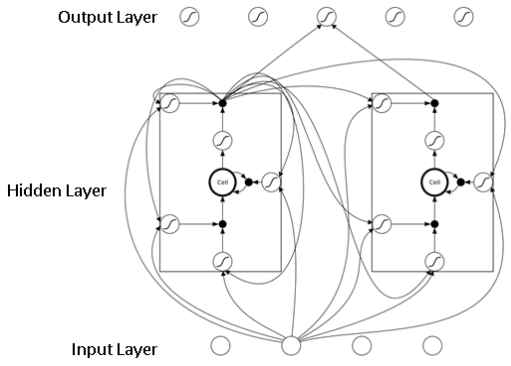

Considering a network with H hidden nodes and time series input given by x_i^t where t is the time and i is the input unit from I inputs, w_{ij} is the weight from unit i to unit j, the input to the unit j at time t is a_j^t and the activation of the unit j in time t is b_j^t, then the indexes ι, ϕ and ω respectively represent the input gate, the output gate and the forget gate, while s_c represents the cell state. Functions f and g could be sigmoid function or the hyperbolic tangent. The feedfoward pass of the network is given by (1) to (9).

* The National Council for Technological and Scientific Development (CNPq) has supported this study.

J. Machado was with the Sul-Riograndense Federal Institute of Technology (IFSul), Charqueadas, RS, Brazil; e-mail: julianomachado@charqueadas.ifsul.edu.br).

V. Cene was with the Postgraduate Program in Electrical Engineering, Federal University of Rio Grande do Sul (UFRGS), researcher of Electrical-Electronic Instrumentation Laboratory (IEE), RS, Brazil (e-mail: vinicius.cene@gmail.com)

A. Balbinot was with the Postgraduate Program in Electrical Engineering, Federal University of Rio Grande do Sul (UFRGS), coordinator of Electrical-Electronic Instrumentation Laboratory (IEE), RS, Brazil (e-mail: alexandre.balbinot@ufrgs.br)

978-1-5386-1311-5/19/$31.00 ©2019 IEEE

Input gates:

$$a_t^t = \sum_{i=1}^{I} w_{it} x_i^t + \sum_{h=1}^{H} w_{ht} b_h^{t-1} \quad (1)$$

$$b_t^t = f(a_t^t) \quad (2)$$

Forget gates:

$$a_\phi^t = \sum_{i=1}^{I} w_{i\phi} x_i^t + \sum_{h=1}^{H} w_{h\phi} b_h^{t-1} \quad (3)$$

$$b_\phi^t = f(a_\phi^t) \quad (4)$$

State of the Cells:

$$a_c^t = \sum_{i=1}^{I} w_{ic} x_i^t + \sum_{h=1}^{H} w_{hc} b_h^{t-1} \quad (5)$$

$$s_c^t = b_\phi^t s_c^{t-1} + b_t^t g(a_c^t) \quad (6)$$

Output Gates:

$$a_\omega^t = \sum_{i=1}^{I} w_{i\omega} x_i^t + \sum_{h=1}^{H} w_{h\omega} b_h^{t-1} \quad (7)$$

$$b_\omega^t = f(a_\omega^t) \quad (8)$$

Cell output

$$b_c^t = b_\omega^t g(s_c^t) \quad (9)$$

This work aims to show an estimator for a sEMG virtual channel based on the information from another set of sEMG channels that were acquired simultaneously with a Recurrent Neural Network (RNN) by using nodes in the hidden layer based in Long Short-Term Memory (LTSM) cells. The work of [11] shows that a Time-Varying Auto Regressive Moving Average (TVARMA) model of a virtual sEMG sensor, in fault tolerance approaches, could improve the classification hit rate in the presence of noisy sEMG channels, with the virtual sensors replacing the noisy ones.

II. Methods

The methodology applied to this work aimed to demonstrate how a Support Vector Machine (SVM) classifies sEMG signals when one of the channels is replaced by a virtual one estimated by an RNN-LSTM. Results are computed based on the average of the hit rate for each selected healthy volunteer of the database.

A. NinaPro sEMG Database

The publicly available NINAPro (Non-Invasive Adaptive Prosthetics) database of sEMG signals was used in this study. The NINAPro database uses 12 active wireless electrodes of the DelsysTM TrignoWireless System® [19]. The NINAPro data is acquired through the National Instruments NI-DAQ PCMCIA 6024E platform at a rate of 2 kHz, 12 bits and with a noise lower than 750nV RMS [20]. It is important to highlight that this study does not use any feedback system and does not monitor the force neither the way the user performs the movements.

The sEMG database of each subject consists of one session that contains 102 movements. Each one of seventeen distinct movements is repeated 6 consecutive times separated by rest times. The sEMG data is acquired through 12 surface electrodes. The twelve electrodes are divided into eight electrodes uniformly spaced just beneath the elbow at a fixed distance from the radio-humeral joint, two electrodes on the flexor digitorum and the extensor digitorum, and two electrodes on the main activity spots of the biceps and the triceps.

The analyzed movements can be seen in the respective order in Fig. 2: thumb up; thumb flexed over ring and little finger; flexion of ring and little finger; thumb flexion; fingers abduction; fingers flexed together; pointing index; fingers closed together; wrist supination and pronation (rotation axis through the middle finger); wrist supination and pronation (rotation axis through the little finger); wrist flexion and extension; wrist radial and ulnar deviation; and wrist extension with closed hand.

Figure 2: The analyzed movements. Adapted from [21].

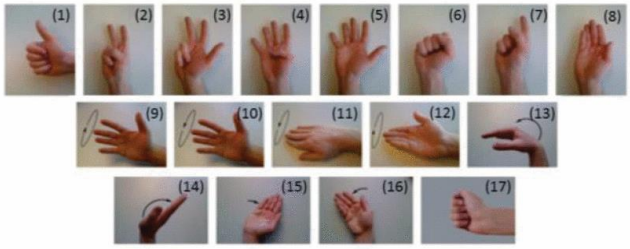

B. Pre-Processing and Feature Extraction

In this step, the signals are filtered, rectified and normalized. Afterwards, the data set is divided into different segments of sliding windows, which are overlapping as explained in [22]. For each analyzed window, one feature was extracted and computed to be the data input of the RNN-LSTM regressor and the SVM classifier.

A digital band-pass filter of order 20 applied to a frequency ranging from 20 to 500 Hz was used in the signals. The sampling frequency was of 2 kS/s. The normalization was performed separately for each channel, and all signal database was used for the session.

A 300 ms length sliding window with increments of 75 ms (25%) was used. For window analyzed size, the Root Mean Square (RMS) of the signals was extracted for the characterization of the muscle contraction.

C. Virtual Channel Estimation and Data Classification

The virtual channel data was estimated with a RNN with four layers: sequence input, LSTM with 50 hidden nodes, fully connected and regression. The movements were classified by a SVM with a radial basis kernel function to better fit nonlinear data [23] and an one-versus-all output, in three distinct cases: 1) with the original data; 2) with one of the channels contaminated with saturation; 3) with one of the channels replaced by a virtual channel.

The SVM and RNN-LSTM training was held by using 70% of the balanced data for all 17 classes and the results for the 30% remaining data are presented below. The process involved 10 individuals from the database, and parameters were trained for each individual. The same data was used to train the SVM and the RNN-LSTM as the data used to test the SVM was considered to regress the virtual channel test data. All the codes and results are evaluated in the *Matlab*® 2018a.

III. Results and Discussion

Results per channel (Ch) are summarized in Table 1. First column (U) shows the average hit rate from all the 10 subjects for the 17 movements with uncontaminated data. Second column (S) presents the average classification hit rate for a single channel with artificial saturation contamination, as described in [24]. And the third column (V) shows the average hit rate for the virtual channel estimated by the RNN-LSTM, with the eleven remaining channels.

The virtual channels have highly improved the classification hit rate, which is degraded by saturation data therefore showing that the system can adapt to a fault sensor using a RNN-LSTM to regress the contaminated channel without the need of retraining, as the RNN-LSTM parameters could be storage in a memory device. As the RNN-LSTM shares many parameters [18], this could be a viable solution to embedded devices.

TABLE I. Results of the sEMG data classification from uncontaminated Channel (U), Saturated Channel (S) and Virtual Channel (V) for each of the 12 Channels (Ch)

U	S	V	Ch
73.96% ± 3.02%	9.29% ± 4.42%	66.48% ± 6.11%	1
	6.75% ± 1.12%	66.56% ± 4.85%	2
	8.28% ± 1.83%	65.03% ± 5.39%	3
	7.21% ± 1.62%	68.31% ± 3.61%	4
	6.28% ± 0.46%	68.36% ± 4.48%	5
	6.72% ± 1.06%	67.01% ± 4.16%	6
	7.26% ± 1.14%	66.21% ± 5.27%	7
	7.80% ± 1.17%	63.55% ± 4.89%	8
	7.57% ± 1.84%	67.41% ± 5.66%	9
	8.48% ± 3.47%	65.83% ± 2.54%	10
	9.07% ± 3.52%	60.76% ± 6.16%	11
	7.59% ± 3.37%	61.90% ± 5.74%	12

IV. Conclusions

The improved classification hit rate has shown that the virtual sensor is better than the saturation channel for the 10 healthy subjects selected from the NinaPro database. The saturation data is practically uncorrelated with the sEMG data from the channels therefore causing the degradation of the classifier. The virtual channel, estimated by the remaining sEMG channels, is probably highly correlated to the information, due to the natural crosstalk between the muscles EMG signals. To further studies, a greater number of contaminated channels might show the limitations of the RNN-LSTM, and different types of noise could make it clear when the virtual channel is needed. [11]. Different RNN-LSTM architectures could show a better predict data therefore significantly improving the classification hit hate with the virtual channel. An experimental statistical analysis is needed, as well as the study with amputated subjects.

References

[1] M. Atzori, H. Muller, and M. Baechler, "Recognition of hand movements in a trans-radial amputated subject by sEMG," in *2013 IEEE 13th International Conference on Rehabilitation Robotics (ICORR)*, 2013, pp. 1–5.

[2] A. Balbinot, G. Favieiro, A. Balbinot, and G. Favieiro, "A Neuro-Fuzzy System for Characterization of Arm Movements," *Sensors*, vol. 13, no. 2, pp. 2613–2630, Feb. 2013.

[3] N. V. Iqbal, K. Subramaniam, and S. A. P., "A Review on Upper-Limb Myoelectric Prosthetic Control," *IETE Journal of Research*, vol. 64, no. 6, pp. 1–13, 02-Nov-2017.

[4] N. Jiang and D. Farina, "Myoelectric control of upper limb prosthesis: current status, challenges and recent advances," *Front. Neuroeng.*, vol. 7, 2014.

[5] X. Zhang and H. Huang, "A real-time, practical sensor fault-tolerant module for robust EMG pattern recognition," *J. Neuroeng. Rehabil.*, vol. 12, no. 1, p. 18, Feb. 2015.

[6] V. H. Cene, G. Favieiro, and A. Balbinot, "Upper-limb movement classification based on sEMG signal validation with continuous channel selection," in *2015 37th Annual International Conference of the IEEE Engineering in Medicine and Biology Society (EMBC)*, 2015, pp. 486–489.

[7] J. I. Furukawa, T. Noda, T. Teramae, and J. Morimoto, "Estimating joint movements from observed EMG signals with multiple electrodes under sensor failure situations toward safe assistive robot control," in *Proceedings - IEEE International Conference on Robotics and Automation*, 2015, vol. 2015–June, no. June, pp. 4985–4991.

[8] T. A. Kuiken, G. A. Dumanian, R. D. Lipschutz, L. A. Miller, and K. A. Stubblefield, "The use of targeted muscle reinnervation for improved myoelectric prosthesis control in a bilateral shoulder disarticulation amputee.," *Prosthet. Orthot. Int.*, vol. 28, no. 3, pp. 245–53, Dec. 2004.

[9] G. Cheron, F. Leurs, A. Bengoetxea, J. P. Draye, M. Destrée, and B. Dan, "A dynamic recurrent neural network for multiple muscles electromyographic mapping to elevation angles of the lower limb in human locomotion," *J. Neurosci. Methods*, vol. 129, no. 2, pp. 95–104, Oct. 2003.

[10] A. Bengoetxea *et al.*, "Physiological modules for generating discrete and rhythmic movements: action identification by a dynamic recurrent neural network," *Front. Comput. Neurosci.*, vol. 8, Sep. 2014.

[11] K. de O. A. De Moura and A. Balbinot, "Virtual sensor of surface electromyography in a new extensive fault-tolerant classification system," *Sensors (Switzerland)*, vol. 18, no. 5, p. 1388, May 2018.

[12] N. Bu, O. Fukuda, and T. Tsuji, "EMG-based motion discrimination using a novel recurrent neural network," *J. Intell. Inf. Syst.*, vol. 21, no. 2, pp. 113–126, 2003.

[13] D. E. Rumelhart, G. E. Hinton, and R. J. Williams, "Learning representations by back-propagating errors," *Nature*, vol. 323, no. 6088, pp. 533–536, Oct. 1986.

[14] I. Goodfellow, Y. Bengio, and A. Courville, *Deep learning*. Cambridge, US: MIT Press, 2016.

[15] A. Graves, *Supervised Sequence Labelling with Recurrent Neural Networks*, vol. 385. Springer, 2012.

[16] S. Hochreiter, Y. Bengio, P. Frasconi, and J. Schmidhuber, "Gradient Flow in Recurrent Nets: the Difficulty of Learning Long-Term Dependencies," in *A Field Guide to Dynamical Recurrent Networks*, J. F. Kolen and S. C. Kremer, Eds. Wiley-IEEE Press, 2001, p. 464.

[17] S. Hochreiter and J. Schmidhuber, "Long Short-Term Memory," *Neural Comput.*, vol. 9, no. 8, pp. 1735–1780, Nov. 1997.

[18] F. A. Gers, J. Schmidhuber, and F. Cummins, "Learning to forget: Continual prediction with LSTM," *Neural Comput.*, vol. 12, no. 10, pp. 2451–2471, Oct. 2000.

[19] A. Gijsberts, M. Atzori, C. Castellini, H. Müller, and B. Caputo, "Movement error rate for evaluation of machine learning methods for sEMG-based hand movement classification," *IEEE Trans. Neural Syst. Rehabil. Eng.*, vol. 22, no. 4, pp. 735–744, Jul. 2014.

[20] M. Atzori *et al.*, "Electromyography data for non-invasive naturally-controlled robotic hand prostheses," *Sci. Data*, vol. 1, p. 140053, Dec. 2014.

[21] M. Atzori *et al.*, "Characterization of a benchmark database for myoelectric movement classification," *IEEE Trans. Neural Syst. Rehabil. Eng.*, vol. 23, no. 1, pp. 73–83, 2015.

[22] K. Englehart and B. Hudgins, "A robust, real-time control scheme for multifunction myoelectric control," *IEEE Trans. Biomed. Eng.*, vol. 50, no. 7, pp. 848–854, Jul. 2003.

[23] J. Chorowski, J. Wang, and J. M. Zurada, "Review and performance comparison of SVM- and ELM-based classifiers," *Neurocomputing*, vol. 128, pp. 507–516, 2014.

[24] P. McCool, G. D. Fraser, A. D. C. Chan, L. Petropoulakis, and J. J. Soraghan, "Identification of contaminant type in surface electromyography (EMG) signals," *IEEE Trans. Neural Syst. Rehabil. Eng.*, vol. 22, no. 4, pp. 774–783, Jul. 2014.